PNNL-11037

UC-~~810~~ 2000

Project Technical Information

Development of Models and Software for Liquidus Temperatures of Glasses of HWVP Products: Final Report

P. R. Hrma
J. D. Vienna
A. D. Pelton
P. Wu
G. Eriksson
S. Degtiarev

March 1996

Prepared for the U.S. Department of Energy
under Contract DE-AC06-76RLO 1830

Pacific Northwest National Laboratory
Operated for the U.S. Department of Energy
by Battelle Memorial Institute

Battelle

PNNL-11037
UC-810
Project Technical Information

Development of Models and Software for Liquidus Temperatures of Glasses of HWVP Products: Final Report

P. R. Hrma
J. D. Vienna
A. D. Pelton*
P. Wu*
G. Eriksson*
S. Degtiarev*

March 1996

Prepared for
the U.S. Department of Energy
under Contract DE-AC06-76RLO 1830

Pacific Northwest National Laboratory
Richland, Washington 99352

*Centre for Research in Computational Thermochemistry, Ecole Polytechnique
Montreal, Quebec, Canada

Reprint of historical document PVTD-C95-02.01Q, dated September 1995. Prepared for PNL by the Centre for Research in Computational Thermochemistry, Ecole Polytechnique, Montreal, Quebec, Canada. Data, formatting, and other conventions reflect standards at the original date of printing. Technical peer reviews and editorial reviews may not have been performed.

DISCLAIMER

PACIFIC NORTHWEST NATIONAL LABORATORY
operated by
BATTELLE
for the
UNITED STATES DEPARTMENT OF ENERGY
under Contract DE-AC06-76RLO 1830

Printed in the United States of America

Available to DOE and DOE contractors from the
Office of Scientific and Technical Information, P.O. Box 62, Oak Ridge, TN 37831;
prices available from (615) 576-8401.

Available to the public from the National Technical Information Service,
U.S. Department of Commerce, 5285 Port Royal Rd., Springfield, VA 22161

The document was printed on recycled paper.

TABLE OF CONTENTS

1 INTRODUCTION/SUMMARY

In an earlier report [92 Pel] was described the development of software and thermodynamic databases for the calculation of liquidus temperatures of glasses of HWVP products containing the components SiO_2-B_2O_3-Na_2O-Li_2O-CaO-MgO-Fe_2O_3-Al_2O_3-ZrO_2-"others".

The software package developed at that time consisted of the EQUILIB program of the F*A*C*T computer system with special input/output routines. Since then, Battelle has purchased the entire F*A*C*T computer system, and this fully replaces the earlier package. Furthermore, with the entire F*A*C*T system, additional calculations can be performed such as calculations at fixed O_2, SO_2, etc. pressures, or graphing of output. Furthermore, the public F*A*C*T database of over 5 000 gaseous species and condensed phases is now accessible.

The private databases for the glass and crystalline phases were developed for Battelle by optimization of thermodynamic and phase diagram data. That is, all available data for 2- and 3-component sub-systems of the 9-component oxide system were collected, and parameters of model equations for the thermodynamic properties were found which best reproduce all the data. For representing the thermodynamic properties of the glass as a function of composition and temperature, the modified quasichemical model was used. This model was described in the earlier report [92 Pel] along with all the optimizations. With the model, it was possible to predict the thermodynamic properties of the 9-component glass, and thereby to calculate liquidus temperatures. Liquidus temperatures measured by Battelle for 123 CVS glass compositions were used to test the model and to refine the model by the addition of further parameters.

In the present report, we describe the continuation of this work.

First, the optimization of the base 9-component glass was extensively re-examined and improved as will be discussed in Section 2. Many binary and ternary systems were completely re-optimized, and our treatment of Al_2O_3 and Fe_2O_3 in the model was revised to better account for the charge compensation effect. The clinopyroxene phase has now been modeled as a solid solution $NaFeSi_2O_6$-$CaMgSi_2O_6$ and new thermodynamic data for acmite have been used. A sodium-calcium silicate solid solution has also been included, as has the compound $Na_2ZrSi_2O_7$.

Chrome, nickel, manganese and Fe^{2+} were added to the database through optimization of a large amount of data as described below in Section 3-6. A model for the corundum solid solution (Cr_2O_3-Fe_2O_3-Al_2O_3) was also developed. Data for Cr, Ni and Fe in other solid compounds and solutions were also optimized, but these phases were never calculated to form as primary phases over the range of composition of the CVS glasses and so they were not included in the databases prepared for Battelle.

A model was also developed for the (Fe, Ni, Mn)(Fe, Al, Cr, Mn)$_2O_4$ spinel phase, and parameters were obtained by optimization as discussed in Section 8.

Calculated liquidus temperatures and primary phases are compared with the experimental results in Section 7. Agreement is significantly improved over that in the earlier report. The comparison of calculations and experimental results is discussed in detail in Section 7.1. Comparisons of calculated and experimental spinel liquidus temperatures are discussed in Section 8.

Bi was not added to the database as originally proposed because, following discussions with P. Hrma, it was decided to include Mn in the spinel model instead.

A model for sulfate, phosphate, chloride, fluoride, iodide and water in dilute solutions (<10 wt.%) in glass was developed. This required re-programming of a number of F*A*C*T software modules.

Calculations of the solubilities of these constituents are compared to available data in Section 9. Agreement is generally very good, and in most cases this agreement is achieved with no adjustable parameters. Solubilities in equilibrium with a gas phase (containing SO_2, O_2 H_2O, etc.) can be calculated with the ACT option of the EQUILIB program. Solubilities in equilibrium with solid or liquid sulphates, phosphates and halides can also be calculated. In the case of phosphates, optimized data for the solid phosphates are included in Battelle's private one-component database. For liquid sulphates and halides, which can form molten salt solutions, use either the /SOLN-SALT/ solution from the public F*A*C*T database, or the Li, Na, Mg, Ca/F, SO_4 molten salt solution which has been prepared by optimization and is included in the private SOLUTION database. Data for pure solid and liquid sulfates and halides can be taken from the public F*A*C*T database.

The optimization of the Li, Na, Mg, Ca/F, SO_4 molten salt phase is discussed in Section 10.

A list of the solutions in the optimized private SOLUTION database which has been prepared is given in Table 1, while a list of the contents of the private one-component databases prepared for Battelle is given in Table 2. In the species selection step of the EQUILIB program one should select only these solutions and compounds as well as the /SOLN-SALT/ phase and, if required, data for pure liquid or solid halides and sulfates and any gases from the public F*A*C*T databases. No other species or solutions from the public F*A*C*T databases should be required, and their selection could cause problems of compatibility of data. Of course, a saving in computation time can be realized if species which are certain not to form in a given case are not selected. Note also that after an EQUILIB calculation, if one enters "LIST", then the calculated activities of all species and solution components are displayed.

Table 1

Solutions in Private Battelle Database

```
FILE    1         DEC 14, 1994
NaCa silicate solid solution (Na2Ca2Si3O9-Na4CaSi3O9)

FILE    2         JAN 11, 1995
Acmite-Augite solid solution (NaFeSi2O6-CaMgSi2O6)

FILE    3     MON APR 11, 1994
Corundum Al2O3-Cr2O3-Fe2O3 solid solution

FILE    4         AUG 31, 1995
Spinel (Fe,Ni,Mn)(Fe,Cr,Al,Mn)2O4

FILE    5         AUG 28, 1995
Salt-liquid Li,Na,Mg,Ca/F,SO4

FILE    6     TUE AUG 29, 1995
Glass

FILE    7     TUE AUG 29, 1995
Mn2SiO4-Mg2SiO4  solid solution
```

Table 2

Compounds in Private Battelle Database

```
Species found in USERBASE

B2O3                              : S1  L1
Na2O                              : S1  S2  S3  L1
Mg*O                              : S1  L1  G1
Al2O3                             : S1  S2  S3  S4  L1
Si*O2                             : S1  S2  S3  S4  S5  S6  L1
Li2Si*O3                          : S1
Mg2Si*O4                          : S1
Li*Al*Si2O6                       : S1
Na*Al*Si*O4                       : S1
Na*Al*Si3O8                       : S1  S2
Li3(P*O4)                         : S1
Na3(P*O4)                         : S1
Ca*O                              : S1  L1  G1
NA4CA*SI3O9                       : S1
NA2CA2SI3O9                       : S1
NA2CA3SI6O16                      : S1
MG*CA*SI2O6                       : S1
Ca*Al2Si2O8                       : S1
Ca3(P*O4)2                        : S1  S2
Cr2O3                             : S1  L1
Mn*Si*O3                          : S1
Mn2Si*O4                          : S1  L1
Fe2O3                             : S1  S2
Fe3O4                             : S1  S2  L1
Na*Fe*Si2O6                       : S1
Zr*O2                             : S1  S2  S3  L1  G1
Zr*Si*O4                          : S1
Na2Zr*Si2O7                       : S1
```

2 OPTIMIZATION OF BASE GLASS

The optimization of the base glass (SiO_2-B_2O_3-Na_2O-Li_2O-CaO-MgO-Fe_2O_3-Al_2O_3-ZrO_2) was discussed in the earlier report [92 Pel]. Since then, the optimization has been extensively re-examined and improved.

A number of ternary sub-systems have been re-optimized with attention paid only to those composition regions where the basicity falls within the range of basicities of Battelle's CVS glasses because, from the equations of the model, only optimizations within these composition regions will have any influence on the multicomponent calculations. According to the model, "basicity" is defined as:

$$(n_{SiO_2}+2n_{B_2O_3}+n_{ZrO_2})/(n_{SiO_2}+2n_{B_2O_3}+n_{ZrO_2}+2n_{Na_2O}+2n_{Li_2O}+n_{CaO}+n_{MgO}+2n_{Al_2O_3}+2n_{Fe_2O_3})$$

2.1 Na_2O-B_2O_3-SiO_2 system

In the case of the Na_2O-B_2O_3-SiO_2 system, the following optimized parameters were obtained. Calculated and experimental [51 Mor] liquidus points are compared in Table 3.

Since the optimization only applies for the range of basicity of the CVS glasses, the miscibility gap at low Na_2O contents in the Na_2O-B_2O_3-SiO_2 system is not correctly reproduced.

$$\omega^{61}_{NaSi\,(B)} = -83.68 \text{ kJ/mol}$$

$$\omega^{11}_{SiNa\,(B)} = -125.52 \text{ kJ/mol}$$

$$\omega^{01}_{NaB\,(Si)} = 75.31 \text{ kJ/mol}$$

Table 3

Calculated and Experimental [51 Mor] Liquidus Points in the Na_2O-B_2O_3-SiO_2 System

Point Number (from [51 Mor])	Composition (wt.%)			T(°C)	
	Na_2O	B_2O_3	SiO_2	expt.	calc.
102	30.8	15.8	53.4	706	680
104	28.3	11.4	60.3	710	687
105	30.0	10.0	60.0	755	722
106	34.0	6.0	60.0	805	797
107	49.2	21.2	29.6	854	869
108	49.4	15.2	35.4	916	949
109	49.7	10.3	40.0	966	1002
110	35.9	15.4	48.7	769	712
111	42.0	18.2	39.8	784	779
87	16.3	30.5	47.2	787	835
89	22.0	28.0	50.0	760	736
90	19.0	26.3	54.7	771	812
92	21.0	23.6	55.4	784	778
93	26.5	12.9	60.6	676	671

2.2 Na_2O-Al_2O_3-SiO_2 system

In the Na_2O-Al_2O_3-SiO_2 system, a "charge compensation effect" is operative, whereby an Al atom can replace Si on a network site only if paired with a Na ion. This means that the structure and properties of the glasses are very different on either side of a line where the Na/Al molar ratio is 1.0. Since this ratio is greater than 1.0 for nearly all CVS glasses, it was decided to optimize only this region. This was found to be much easier if the quasichemical "charge parameter" of alumina was set equal to that of sodium (0.3444). Furthermore, since compositions on the Al_2O_3-SiO_2 and Na_2O-Al_2O_3 systems are not in the ranges of composition (either of Na/Al ratio or of basicity) of interest, the binary parameters of these systems were chosen only with a view to optimizing the ternary system. The following optimized parameters were obtained

$$\omega_{NaAl} = -449.78 \text{ kJ/mol}$$
$$\omega_{AlSi} = -190.255\, y_{Si}^{7} \text{ kJ/mol}$$
$$\omega_{NaAl(Si)}^{01} = -167.36 \text{ kJ/mol}$$

A comparison of calculated and experimental [60 Osb] invariant points is given in Table 4.

A satisfactory optimization of the nepheline ($NaAlSiO_4$) liquidus of the Na_2O-Al_2O_3-SiO_2 system was not obtained. Consequently, liquidus temperatures of CVS glasses with compositions for which nepheline is a possible primary phase are not well calculated as will be discussed in Section 7.

2.3 Na_2O-Fe_2O_3-SiO_2 system

In the Na_2O-Fe_2O_3-SiO_2 system, a charge compensation effect is also probably operative, although to a leaser degree than in Na_2O-Al_2O_3-SiO_2. In any case, the optimization of this system was improved over that reported in the earlier report by setting the "charge parameter" of $FeO_{3/2}$ equal to that of Na_2O (0.3444). Furthermore, most emphasis was placed on fitting the phase diagram [30 Bow] at low Fe_2O_3 contents. More recent data [90 Hol] for the thermodynamic properties of pure acmite ($NaFeSi_2O_6$) were employed than were used in the earlier report. ΔH_{298}° of acmite was later adjusted by -16.75 kJ/mol in the optimization which is within the experimental error limits. One optimized ternary parameter was required:

$$\omega_{NaSi(Fe)}^{01} = -50.21 \text{ kJ/mol}$$

Table 4

Comparison of Calculated and Experimental [60 Osb] Invariant Points in the Na_2O-Al_2O_3-SiO_2 System

Composition (wt.%)				T(°C)	Reaction
	Na_2O	Al_2O_3	SiO_2		
expt. calc.				1062 1073	L → SiO_2 + $NaAlSi_3O_8$
expt. calc.				740 750	L → $Na_2Si_2O_5$ + SiO_2 + $NaAlSi_3O_8$
expt. calc.	26.0 27.8	12.5 11.2	61.5 61.0	732 735	L → $Na_2Si_2O_5$ + $NaAlSi_3O_8$ + $NaAlSiO_4$
expt. calc.	32.0 31.5	10.1 10.4	57.9 58.1	760 742	L → $Na_2Si_2O_5$ + Na_2SiO_3 + $NaAlSiO_4$
expt. calc.				1118 1118	L → $NaAlSi_3O_8$

2.4 Other Systems with Al_2O_3 and Fe_2O_3

The treatment of the components Al_2O_3 and Fe_2O_3 is now different, since their assumed "charge parameters" in the quasichemical model were changed in order to give better optimizations of the important Na_2O-Al_2O_3-SiO_2 and Na_2O-Fe_2O_3-SiO_2 systems. (These systems are important because Na_2O and SiO_2 are both major CVS glass components.) Because of this, it was necessary to re-optimize all systems containing Al_2O_3 or Fe_2O_3. The systems which were re-optimized are: CaO-Fe_2O_3, Al_2O_3-B_2O_3, Al_2O_3-CaO, Al_2O_3-MgO, Al_2O_3-ZrO_2, Na_2O-Fe_2O_3, SiO_2-Fe_2O_3, Al_2O_3-B_2O_3-SiO_2, Al_2O_3-Li_2O-SiO_2, CaO-Al_2O_3-SiO_2, MgO-Al_2O_3-SiO_2.

2.5 Na_2O-ZrO_2-SiO_2 system (and compound $Na_2ZrSi_2O_7$)

Very few data are available for this system, but a value of $\omega^{21}_{NaSi\,(Zr)} = -209.2$ kJ/mol (- 50 kcal/mol) was estimated. A compound $Na_2ZrSi_2O_7$ has been observed which was not included in our earlier report [92 Pel]. No thermodynamic data are available for this compound. Accordingly, Cp was estimated from Cp of ZrO_2 and $ZrSiO_4$, while ΔH°_{298} and S°_{298} were chosen to best reproduce the observed liquidus temperatures of the CVS glasses.

2.6 Na_2O-CaO-SiO_2 system (and solid solution $Na_2Ca_2Si_3O_9$-$Na_4CaSi_3O_9$)

The earlier optimization of this system has been improved. In particular, the assumption of an ideal solid solution between $Na_2Ca_2Si_3O_9$ and $Na_4CaSi_3O_9$ markedly improves the agreement between the calculations and the published phase diagram.

2.7 Clinopyroxene ($NaFeSi_2O_6$-$CaMgSi_2O_6$) solid solution

A major improvement in reproducing the observed liquidus temperatures of the CVS glasses was effected by treating the clinopyroxene phase as a solid solution of 1/2($NaFeSi_2O_6$) and 1/2($CaMgSi_2O_6$). Thermodynamic data for pure $CaMgSi_2O_6$ were taken from the F*A*C*T database, and a Henrian solution parameter

$$RT\ln \gamma_{1/2(CaMgSi_2O_6)} = -26342 + 19.246\,T \text{ J/mol}$$

was chosen to best reproduce the observed CVS glass liquidus points.

Although Cr and Ni can probably also dissolve in this solid solution, this was not considered in the present model because of lack of data and because good results were obtained in most cases without this.

2.8 Optimization of CVS liquidus calculations

In many cases, interactions between minor constituents of the CVS glasses can be important. For example, an $\omega_{ZrSi(Al)}$ ternary parameter is necessary in the calculations. However this parameter cannot be obtained by simply optimizing data for the ZrO_2-SiO_2-Al_2O_3 ternary system because ZrO_2 and Al_2O_3 are minor constituents of the glasses, and the interactions between these constituents in a predominantly sodium borosilicate glass is quite different from that in a ZrO_2-SiO_2-Al_2O_3 glass. Consequently, it is only possible to optimize such parameters from actual measurements on the CVS glasses. In this way the following parameters were determined:

$$\omega^{01}_{ZrSi\,(Al)} = -313.80 \text{ kJ/mol}$$
$$\omega^{21}_{LiSi\,(Zr)} = -138.07 \text{ kJ/mol}$$
$$\omega^{01}_{CaSi\,(B)} = 62.76 \text{ kJ/mol}$$
$$\omega^{01}_{BSi\,(Zr)} = -12.55 \text{ kJ/mol}$$
$$\omega^{01}_{LiSi\,(Ca)} = -100.42 \text{ kJ/mol}$$
$$\omega^{01}_{MgSi\,(Zr)} = 167.36 \text{ kJ/mol}$$
$$\omega^{01}_{CaSi\,(Zr)} = -41.84 \text{ kJ/mol}$$
$$\omega^{01}_{CaSi\,(Fe)} = -87.86 \text{ kJ/mol}$$
$$\omega^{01}_{FeSi\,(Mg)} = 16.74 \text{ kJ/mol}$$

3 INCLUDING Fe^{2+} IN THE DATABASES

Optimizations were performed for the liquid and sollid phases of the FeO-Fe_2O_3-SiO_2-CaO system. An article on this work is in preparation. The following systems involving Fe^{2+} were also optimized: FeO-MgO, FeO-ZrO_2, FeO-Al_2O_3-SiO_2. All these optimizations will appear in "Phase Diagrams for Ceramists". No data for the FeO-B_2O_3 system could be found, so ideal mixing was assumed.

The optimized parameters have been incorporated into the database for the glass and can be used to calculate the effect of oxygen pressure on the Fe^{2+}/Fe^{3+} ratio in the glass (using the EQUILIB program and the ACT option).

Fe^{2+} has also been incorporated into the database for the spinel phase as discussed in Section 8.

Data for Fe^{2+} in solid crystalline phases and solid solutions such as Fe_2SiO_4-M_2SiO_4 or $FeSiO_3$-$MSiO_3$ solutions (M = Mg, Ca) were also optimized, but these phases were never found to form as primary phases from the CVS glasses in the calculations and so they have not been included in the database prepared for Battelle.

4 INCLUDING CHROME IN THE DATABASES

Most binary, ternary and quaternary sub-systems of the $CrO-Cr_2O_3-SiO_2-CaO-Al_2O_3-FeO-Fe_2O_3$ system have been fully optimized. Two articles are being prepared based on this work. As well, the optimizations will appear in "Phase Diagrams for Ceramists". Good quantitative reproduction of all phase diagram and thermodynamic data has been obtained, including the effect of O_2 pressure on the Cr^{2+}/Cr^{3+} ratio and on the phase equilibria.

Data for several Cr-containing solid phases were also optimized. The spinel phase is discussed in Section 8. A database was prepared for the corundum solid solution, $Fe_2O_3-Al_2O_3-Cr_2O_3$. This phase was found in the calculations to be the primary phase for certain CVS glasses. None of the other Cr-containing solid phases were found to form as primary phases from the CVS glasses in the calculations, and so they have not been included in the database prepared for Battelle.

No data for the $Na_2O-CrO-Cr_2O_3$ system were found. Consequently, one parameter $\omega_{NaCr[3+]}$ was optimized by using spinel liquidus data for the CVS glasses.

Cr^{6+} has not been included in the database due to lack of available data. This oxidation state will be most important in basic glasses.

5 INCLUDING NICKEL IN THE DATABASES

Parameters from optimizations of the $NiO-SiO_2$, NiO-MgO and NiO-CaO systems were included in the glass database. These optimisations are to be published in "Phase Diagrams for Ceramists". The phase Ni_2SiO_4 was optimized but was found never to appear as a primary phase in the calculaions. Consequently, it has not been included in the database prepared for Battelle. No data for the $Na_2O-B_2O_3-NiO$ system or its sub-systems were found. Hence, an ω_{NaNi} and an ω_{BNi} parameter were optimized by using spinel liquidus data for the CVS glasses. The spinel phase, which contains nickel, is discussed in Section 8.

6 INCLUDING MANGANESE IN THE DATABASES

Parameters obtained by optimizing the following systems were included in the glass database: MgO-MgO, $MnO-SiO_2$, MnO-CaO, $MnO-Al_2O_3$, and $MnO-ZrO_2$. These optimizations will appear in "Phase Diagrams for Ceramists". From an examination of available data it was concluded that Mn^{3+} will not appear in appreciable concentrations in CVS glasses, and so Mn^{3+} was not included in the glass database.

Data for the $MnSiO_3$ solid phase and Mn_2SiO_4-Mg_2SiO_4 solid solutions were also included in Battelle's databases. Although neither of these phases appeared in the calculations for the CVS glasses, they could appear in glasses with somewhat higher Mn contents.

Manganese has been included in the spinel phase as discussed in Section 8.

7 CALCULATIONS FOR CVS GLASSES

Experiments on 123 compositions were carried out by Battelle. The compositions are listed in Table 5. The ID number is that used by Battelle. Glasses 1 to 23 are CVS-I. Glasses 24 to 123 are CVS-II glasses 1 to 100. The compositions of "others" is shown in Table 6 as regards Cr, Ni and Mn content.

Experimental liquidus temperatures, primary phases and the elements observed by SEM/EDS in the primary phases are shown in Table 7 which is reproduced from the most recent tables supplied to us by Battelle in 1994.

Calculated liquidus temperatures and primary phases are shown in Table 8. These were calculated by assuming that no prior precipitation of spinel occurs (that is, it is assumed that the amount of any prior spinel precipitation has a negligible effect on the glass composition). For some glass compositions, the calculations indicated that two immiscible glass phases exist at equilibrium. However, the calculations shown in Table 8 were all performed by assuming only one glass phase. In cases where two glass phases appear at equilibrium, taking account of this fact in the calculations usually only changes the calculated liquidus temperature by 10° or less. In cases where two "primary" phases appear in Table 8, the lower temperature liquidus is a metastable liquidus calculated by suppressing the formation of the phase appearing at the higher temperature.

Note that in Table 8 the "CO(R)" phase is the corundum solid solution (Fe_2O_3-Al_2O_3-Cr_2O_3). Clinopyroxene (Cp) is the $NaFeSi_2O_6$-$CaMgSi_2O_6$ solid solution.

Calculations of the spinel liquidus, also shown in Table 8, are discussed in Section 8.

The amounts of Ni, Cr and Mn in the "others" (as in Table 6) was taken into account in the calculations. The remaining "others" were grouped together as the one fictitious component "In_2O_3" as described in the earlier report [92 Pel]. (This "compound" is included in the glass database but in no solid phases. Its affect is only to lower the activities of the other components. In_2O_3 was chosen because its molecular weight is close to the average of the "others").

Table 5

Compositions of CVS-I and CVS-II Glasses

Composition (weight fraction)										ID
SiO_2	B_2O_3	Na_2O	Li_2O	CaO	MgO	Fe_2O_3	Al_2O_3	ZrO_2	Others	No
.4801	.1142	.1003	.0376	.0275	.0363	.0568	.0636	.0429	.0407	1
.5500	.0500	.0500	.0700	.1000	.0000	.0200	.1500	.0000	.0100	2
.4200	.2000	.0500	.0700	.0000	.0800	.0200	.1400	.0100	.0100	3
.5700	.2000	.0900	.0100	.0200	.0800	.0200	.0000	.0000	.0100	4
.5700	.0500	.0700	.0700	.0000	.0000	.1500	.0800	.0000	.0100	5
.4400	.2000	.0500	.0700	.0000	.0000	.0200	.0000	.1200	.1000	6
.5700	.0500	.0964	.0100	.1000	.0000	.0336	.0000	.1300	.0100	7
.5363	.0500	.0837	.0100	.0000	.0800	.1500	.0000	.0800	.0100	8
.4200	.1962	.0538	.0100	.0000	.0800	.1400	.0000	.0000	.1000	9
.5700	.0851	.0949	.0100	.0000	.0000	.0200	.1200	.0000	.1000	10
.4200	.1549	.0751	.0100	.1000	.0000	.0200	.1400	.0000	.0800	11
.4200	.1764	.0736	.0700	.1000	.0000	.1500	.0000	.0000	.0100	12
.5700	.2000	.1862	.0100	.0000	.0000	.0200	.0038	.0000	.0100	13
.4200	.2000	.1862	.0100	.0000	.0000	.0200	.0238	.1300	.0100	14
.5589	.0500	.1211	.0700	.0000	.0800	.0200	.0000	.0000	.1000	15
.4327	.0500	.1873	.0100	.0000	.0800	.0858	.1442	.0000	.0100	16
.4545	.0500	.1455	.0100	.1000	.0000	.1400	.0000	.0000	.1000	17
.4214	.0500	.1186	.0700	.0200	.0800	.0200	.0000	.1300	.0900	18
.4801	.1142	.1003	.0376	.0275	.0363	.0568	.0636	.0429	.0407	19
.4801	.1142	.1003	.0376	.0275	.0363	.0568	.0636	.0429	.0407	20
.5700	.2000	.0900	.0100	.0200	.0800	.0200	.0000	.0000	.0100	21
.5363	.0500	.0837	.0100	.0000	.0800	.1500	.0000	.0800	.0100	22
.5153	.0956	.1052	.0375	.0289	.0084	.1179	.0456	.0063	.0393	23
.5226	.0874	.0700	.0600	.0000	.0500	.0400	.0800	.0100	.0800	24
.5017	.0700	.0883	.0600	.0700	.0000	.0450	.1100	.0300	.0250	25

Table 5 (continued)

Compositions of CVS-I and CVS-II Glasses

Composition (weight fraction)										ID
SiO_2	B_2O_3	Na_2O	Li_2O	CaO	MgO	Fe_2O_3	Al_2O_3	ZrO_2	Others	No
.4645	.1320	.0700	.0435	.0700	.0100	.0450	.1032	.0368	.0250	26
.5600	.1095	.0700	.0536	.0700	.0000	.0400	.0619	.0100	.0250	27
.4751	.1590	.1010	.0200	.0348	.0000	.0400	.0800	.0100	.0800	28
.5373	.0700	.0700	.0382	.0700	.0046	.1200	.0159	.0100	.0641	29
.4814	.1700	.0700	.0591	.0094	.0000	.0400	.0953	.0100	.0648	30
.5115	.0700	.0985	.0600	.0000	.0500	.1140	.0610	.0100	.0250	31
.5431	.0944	.0924	.0600	.0000	.0000	.0712	.0138	.1000	.0250	32
.4694	.1700	.1306	.0200	.0000	.0000	.0669	.1043	.0100	.0288	33
.4915	.0751	.0833	.0600	.0700	.0100	.0400	.0100	.0935	.0665	34
.4683	.1700	.0700	.0466	.0700	.0100	.0400	.0901	.0100	.0250	35
.4937	.0700	.1692	.0225	.0300	.0500	.0400	.0896	.0100	.0250	36
.4600	.1313	.0802	.0486	.0500	.0200	.0400	.0243	.1000	.0457	37
.4729	.0700	.1700	.0214	.0601	.0000	.0400	.0756	.0100	.0800	38
.5353	.1053	.1125	.0375	.0083	.0084	.0719	.0231	.0385	.0592	39
.4801	.1142	.1003	.0376	.0275	.0363	.0568	.0636	.0429	.0407	40
.5353	.1053	.1125	.0375	.0083	.0084	.0719	.0231	.0385	.0592	41
.5328	.1048	.1129	.0373	.0082	.0084	.0733	.0235	.0392	.0596	42
.5700	.0500	.1031	.0669	.0000	.0000	.0600	.0100	.1300	.0100	43
.5700	.1314	.0500	.0700	.0000	.0800	.0200	.0686	.0000	.0100	44
.5700	.0500	.0735	.0700	.0000	.0800	.0200	.0365	.0000	.1000	45
.5700	.0522	.2000	.0100	.0800	.0000	.0200	.0578	.0000	.0100	46
.4464	.2000	.0736	.0700	.0000	.0000	.0200	.0961	.0000	.0939	47
.5059	.0500	.0841	.0700	.0800	.0000	.1500	.0033	.0000	.0567	48
.4431	.2000	.0512	.0700	.0800	.0000	.0200	.0257	.1000	.0100	49
.5463	.0500	.2000	.0155	.0000	.0800	.0200	.0782	.0000	.0100	50
.5619	.0500	.2000	.0126	.0000	.0000	.0200	.0555	.0000	.1000	51
.4391	.2000	.0675	.0100	.0800	.0000	.0200	.0000	.0834	.1000	52
.5190	.2000	.0832	.0100	.0000	.0000	.1320	.0458	.0000	.0100	53

Table 5 (continued)

Compositions of CVS-I and CVS-II Glasses

Composition (weight fraction)										ID
SiO_2	B_2O_3	Na_2O	Li_2O	CaO	MgO	Fe_2O_3	Al_2O_3	ZrO_2	Others	No
.5700	.1843	.0500	.0331	.0800	.0000	.0200	.0526	.0000	.0100	54
.5445	.0500	.2000	.0428	.0000	.0000	.0200	.0027	.1300	.0100	55
.4200	.0544	.2000	.0364	.0000	.0800	.0200	.0892	.0000	.1000	56
.4200	.1743	.2000	.0369	.0000	.0000	.0200	.1388	.0000	.0100	57
.4200	.0500	.2000	.0428	.0800	.0000	.0632	.1340	.0000	.0100	58
.5421	.0500	.0891	.0700	.0800	.0000	.1500	.0088	.0000	.0100	59
.5700	.0839	.1061	.0700	.0000	.0000	.0200	.1400	.0000	.0100	60
.5147	.1109	.1044	.0100	.0000	.0800	.1428	.0272	.0000	.0100	61
.4838	.0500	.1362	.0700	.0000	.0800	.0742	.0258	.0700	.0100	62
.5040	.0639	.1500	.0421	.0200	.0500	.0200	.1000	.0200	.0300	63
.5325	.0694	.0781	.0700	.0500	.0200	.0300	.1000	.0200	.0300	64
.5675	.0500	.0625	.0700	.0320	.0380	.1000	.0300	.0200	.0300	65
.5070	.1477	.0500	.0653	.0200	.0300	.0300	.0500	.0700	.0300	66
.5700	.1078	.0500	.0699	.0500	.0200	.0200	.0623	.0200	.0300	67
.5299	.1106	.0500	.0595	.0200	.0500	.0308	.0592	.0200	.0700	68
.5264	.1259	.0577	.0700	.0200	.0200	.0200	.0746	.0200	.0654	69
.5294	.0500	.1277	.0429	.0500	.0200	.0200	.0400	.0500	.0700	70
.4700	.1442	.0968	.0390	.0500	.0200	.0200	.0854	.0200	.0546	71
.5073	.1357	.0957	.0413	.0200	.0200	.0515	.0785	.0200	.0300	72
.4801	.1142	.1003	.0376	.0275	.0363	.0568	.0636	.0429	.0407	73
.5328	.1048	.1129	.0373	.0082	.0084	.0733	.0235	.0392	.0596	74
.6000	.0817	.0450	.0788	.0008	.0009	.0720	.0233	.0385	.0590	75
.5226	.0874	.0700	.0600	.0000	.0500	.0400	.0800	.0100	.0800	76
.5328	.1048	.1129	.0373	.0082	.0084	.0733	.0235	.0392	.0596	77
.5328	.1048	.1129	.0373	.0082	.0084	.0733	.0235	.0392	.0596	78
.5328	.1048	.1129	.0373	.0082	.0084	.0733	.0235	.0392	.0596	79
.5328	.1048	.1129	.0373	.0082	.0084	.0733	.0235	.0392	.0596	80

Table 5 (continued)

Compositions of CVS-I and CVS-II Glasses

Composition (weight fraction)										ID
SiO_2	B_2O_3	Na_2O	Li_2O	CaO	MgO	Fe_2O_3	Al_2O_3	ZrO_2	Others	No
.3900	.2000	.0500	.0700	.0200	.0800	.0200	.1500	.0100	.0100	81
.4380	.1718	.1268	.0727	.0375	.0005	.0200	.1150	.0075	.0102	82
.5281	.0876	.1725	.0743	.0063	.0005	.0200	.0925	.0075	.0107	83
.5281	.0664	.1200	.0730	.0000	.0000	.0200	.1625	.0175	.0125	84
.5579	.1765	.1125	.0156	.0500	.0005	.0200	.0500	.0075	.0095	85
.3232	.1717	.1900	.0051	.1000	.0000	.0200	.1800	.0000	.0100	86
.5697	.0509	.0925	.0642	.0025	.0008	.0812	.0288	.0431	.0663	87
.5344	.1128	.0860	.0697	.0007	.0004	.0013	.0196	.1548	.0203	88
.5175	.0917	.1211	.0523	.0097	.0061	.0388	.1180	.0026	.0422	89
.4596	.1587	.1086	.0583	.0024	.0001	.0004	.2043	.0000	.0076	90
.5040	.1355	.0797	.0696	.0007	.0002	.0046	.1640	.0001	.0416	91
.5660	.0781	.0664	.0713	.0079	.0032	.0334	.0816	.0005	.0916	92
.4854	.1418	.0812	.0691	.0008	.0008	.0080	.1819	.0005	.0305	93
.5697	.0509	.0925	.0642	.0025	.0008	.0812	.0288	.0431	.0663	94
.5175	.0917	.1211	.0523	.0097	.0061	.0388	.1180	.0026	.0422	95
.5040	.1355	.0797	.0696	.0007	.0002	.0046	.1640	.0001	.0416	96
.5660	.0781	.0664	.0713	.0079	.0032	.0334	.0816	.0005	.0916	97
.4854	.1418	.0812	.0691	.0008	.0008	.0080	.1819	.0005	.0305	98
.5018	.0600	.1800	.0632	.0400	.0050	.1050	.0200	.0050	.0200	99
.4550	.0600	.1800	.0700	.0050	.0050	.0050	.0200	.1100	.0900	100
.5600	.1600	.0500	.0254	.0050	.0400	.0699	.0200	.0497	.0200	101
.5479	.1600	.0500	.0121	.0050	.0050	.1050	.0200	.0050	.0900	102
.5074	.1600	.0500	.0176	.0050	.0400	.1050	.0200	.0750	.0200	103
.4400	.0600	.1734	.0700	.0050	.0400	.1050	.0200	.0050	.0816	104
.5600	.0950	.1800	.0700	.0050	.0400	.0050	.0200	.0050	.0200	105
.4900	.0951	.1800	.0699	.0400	.0050	.0050	.0200	.0050	.0900	106

Table 5 (continued)

Compositions of CVS-I and CVS-II Glasses

Composition (weight fraction)										ID
SiO_2	B_2O_3	Na_2O	Li_2O	CaO	MgO	Fe_2O_3	Al_2O_3	ZrO_2	Others	No
.4550	.0600	.1800	.0700	.0050	.0050	.1050	.0200	.0800	.0200	107
.4400	.0600	.1800	.0700	.0050	.0200	.0050	.1700	.0050	.0450	108
.4764	.0600	.1800	.0136	.0400	.0050	.0050	.1700	.0050	.0450	109
.4983	.0800	.1800	.0180	.0137	.0050	.0250	.0987	.0613	.0200	110
.4597	.0600	.1403	.0700	.0400	.0050	.0250	.1050	.0750	.0200	111
.4400	.1171	.1800	.0100	.0400	.0050	.1050	.0200	.0629	.0200	112
.5600	.1600	.0542	.0700	.0050	.0050	.1008	.0200	.0050	.0200	113
.5600	.1600	.1050	.0100	.0050	.0400	.0050	.0200	.0050	.0900	114
.4400	.1600	.1000	.0700	.0050	.0400	.0050	.0200	.0700	.0900	115
.4400	.1337	.1279	.0700	.0098	.0050	.0986	.0200	.0050	.0900	116
.4400	.1600	.1800	.0526	.0400	.0050	.0271	.0703	.0050	.0200	117
.463	.109	.163	.042	.010	.016	.087	.032	.004	.074	118
.4801	.1142	.1003	.0376	.0275	.0363	.0568	.0636	.0429	.0407	119
.5328	.1048	.1129	.0373	.0082	.0084	.0733	.0235	.0392	.0596	120
.4200	.1743	.2000	.0369	.0000	.0000	.0200	.1388	.0000	.0100	121
.5203	.0969	.0980	.0356	.0097	.0077	.1019	.0523	.0199	.0577	122
.5329	.0740	.0626	.0596	.0035	.0012	.1229	.0286	.0443	.0704	123

Table 6

Compositions of "Others" in CVS Glasses

ID #	CVS - II #	Composition (wt.%)			
		Cr_2O_3	NiO	MnO_2	Remainder
	55	15	0	47	38
	56	12	0	78	10
	57	9	0	0	91
	64	1.70	14.81	0	83.49
	65	23.7	0	0	76.3
	66	25.5	12.4	34.4	27.7
	67	17.8	0	0	82.2
	68	71.3	0	6.4	22.3
	69	25.93	0	16.32	57.75
	70	38.31	2.69	11.57	47.43
	99	3.47	5.03	8.32	83.18
	100	0.85	9.80	2.98	86.37
All other glasses		2.24	10.30	2.69	84.77

Table 7

Experimental Liquidus Temperatures, Primary Phases, and Elemental Analysis of Primary Phases from Battelle

CVS #	Experimental TI	phase	SEM/EDS elements	TI Spinel	no spinel T range
1	959	ZS		977	
	903	Cp			
2	927	CS	Ca,Si		891-1038
	916	LA	Al,Si		
3	929	Ov	Mg,Si; Fe,Ni		868-1038
4	957	SO	Si		927-1038
5	939	Op	Fe,Si	1035	
6	≥1118	ZS			1014-1118
7	>1118	ZS			1074-1118
	>1118	CZ			
8	>1118	ZS	Zr,Si	>1118	
	>1118	Op	Mg,Si		
9	1097	(?)	Mg,Fe,Si; Cr,Ni	>1118	
10	(?)	(?), severe segregation		>1118	
11	919	CS	Ca,Si; Nd,La	1035	
12	826	Op	Fe,Si		752-1038
13	<571	(None)			571-1038
14	<571	(None)			571-1038
15	866	Ov	Mg,Ni,Si; Cr		837-1038
16	>1118	Ov	Mg,Si	>1118	
17	943	CS	Ca,Si	1000	
	913	Cp	Ca,Fe,Si; Na,Ni		
18	>1118	ZO	Zr		1014-1118
19	916	ZS		961	
	916	Cp	Ca,Mg,Fe,Si; Ni,Cr		
20	913	ZS		966	
	913	Cp			
21	957	SO			927-1038
22	>1118	ZS		>1118	
	>1118	Op			
23	858	Cp		980	
1	929	Ov	Mg,Ni,Si; Fe,Cr	1048	
2	839	CS	Ca,Si		826-928
	800	Cp	Ca,Fe,Ni,Si		

CVS #	Experimental TI	phase	SEM/EDS elements	TI Spinel	no spinel T range
3	931	ZS			782-1038
	887	Cp			
4	810	CS	Ca,Si		702-812
	800	Cp	Ca,Fe,Ni,Si		
5	832	CS	Ca,Si;Zr,Nd,La	988	
6	939	Cp	Ca,Fe,Si; Ni,Cr	>1004	
7	819	Cp	Ca,Fe,Ni,Si	934	
8	866	Op	Fe,Si; Mg	≥1118	
9	1018	ZS			735-1146
10	<585	(None)		>868	
11	1035	ZS	Zr,Si		927-1038
12	840	Cp	Ca,Fe,Mg,Si; Ni,Cr		826-918
13	909	Cp	Ca,Fe,Mg,Si		826-911
14	>1118	ZS			1014-1118
15	<679	(None)		956	
16	877	Cp		906	
17	925	ZS	Zr,Si	971	
	925	Cp	Ca,Mg,Si; Fe		
18	865	Cp	Ca,Fe,Si; Na,Cr,Ni	895	
19	862	Cp	Ca,Na,Fe,Si; Mg,Ni,Cr	>883	
	862	NZ	Na,Zr,Si		
20	1081	ZS	Zr,Si		1012-1115
21	904	Op	Mg,Si		834-951
22	989	Ov	Mg,Ni,Si	994	
23	858	CS	Ca,Si		807-1038
24	<714	(None)		800	
25	899	Op	Fe,Si;Ni	>951	
26	1049	ZS			1012-1115
27	<642	(None)			642-1018
28	<642	(None)			642-872
29	1108	ZS	Zr,Si		1012-1115
30	1070	Hm		1090	
31	939	SO	Si		927-1038
32	1054	NZ	Na;Zr,Si		1008-1114

Table 7 (continued)

Experimental Liquidus Temperatures, Primary Phases, and Elemental Analysis of Primary Phases from Battelle

CVS #	Experimental TI	phase	SEM/EDS elements	TI Spinel	no spinel T range
33	967	Np	Na,Al,Si	>1038	
	967	Ov	Mg,Ni,Si		
34	736	Np	Na,Al,Si		701-872
35	941	Np	Na,Al,Si		895-1115
36	877	Op	Fe,Si		868-1038
37	803	Np	Na,Al,Si		752-1038
38	1042	Ov	Mg,Si; Fe	>1115	
39	1029	ZS			895-1115
40	862	Cp	Ca,Mg,Si; Cr		826-928
41	887	Cp	Ca,Mg,Si; Fe,Ni,Cr		854-936
42	969	Cp	Ca,Fe,Mg,Si	1093	
43	1090	ZS			1012-1115
44	884	Cp	Ca,Mg,Si; Fe,Ni,Cr		807-1038
45	894	Cp	Ca,Mg,Si; Fe,Ni,Cr	>956	
46	858	Cp	Ca,Cr,Fe,Mg,Ni,Si	1004	
47	877	Cp	Ca,Mg,Si; Na,Fe,Ni,Cr		807-1038
48	868	Cp	Ca,Mg,Si; Ni,Fe,Cr		807-1038
49	847	Cp	Ca,Mg,Fe,Si; Ni,Cr	957	
50	922	ZS		1025	
	922	Cp			
51	856	Cp	Ca,Na,Fe,Si; Mg,Cr,Ni	899	
	856	NZ	Na,Zr,Si		
52	973	Op	Fe,Cr,Si	>1038	
53	Radioactive glass -- not measured				
54	Radioactive glass -- not measured				
55	944	CO		>1118	
	906	Cp	Na,Ca,Fe,Cr,Si		
56	880	Cp	Na,Ca,Fe,Cr,Si	1117	
	880	NZ	Na,Zr,Si		
57	1036	CO	Cr;Fe	953	
	945	Cp	Na,Ca,Fe,Cr,Si		
58	906	Ov	Mg,Si; Ni	(?)	
	902	Mg2B2O5(?)	Mg		
59	715	SO	Si		699-1038

Table 7 (continued)

Experimental Liquidus Temperatures, Primary Phases, and Elemental Analysis of Primary Phases from Battelle

CVS #	Experimental TI	phase	SEM/EDS elements	TI Spinel	no spinel T range
60	788	SO	Si		752-966
61	792	SO	Si		717-793
62	<554	(None)			554-1028
63	927	Np	Na,Al,Si		868-1038
64	895	Op	Fe,Si; Cr,Ni	983	
65	>1114	ZS			1066-1114
66	799	Np	Na,Al,Si	>931	
67	1022	CO	Cr		952-1066
68	>1114	CO	Cr		755-874
69	>1114	CO	Cr	>1114	
	983	Op(?)	Cr,Fe,Si		
70	>1114	CO			642-931
	818	LA	Al,Si		
71	890	Op	Fe,Cr,Si	1004	
72	794	Np		>868	
73	816	LA	Al,Si		793-874
74	850	Cp	Ca,Fe,Si; Ni	1066	
75	815	LA	Al,Si		807-1038
76	761	Cp	Ca,Fe,Si; Na		712-924
	744	LS	Si		
77	1027	NZ	Na,Zr,Si		964-1154
78	1129	ZS			1032-1154
79	949	SO	Si	>1154	
80	>1154	ZS	Zr,Si	1129	
81	>1154	(?)	Si	1013	
82	745	LS	Si		693-924
83	741	CS	Ca,Si		719-924
	741	LS	Si		
84	966	NZ	Na,Zr,Si		869-1028
85	>1150	(?)	Si		1042-1154
86	1015	Np	Na,Al,Ca,Si; S,Cr		967-1154
87	<571	(none)			571-874
88	929	ZO			901-1152
89	838	Cp	Ca,Fe,Si; Mg		752-924
90	897	Op	Fe,Si, Cr		841-967
91	886	SO	Si	>967	
92	897	ZS			(?)
93	782	Cp	Na,Ca,Fe,Si	>983	
94	663	CS	Ca Si		642-983
95	804	Cp	Ca,Fe,Si; Na,Mg,Ti		712-924
96	946	ZS		1010	
	946	Cp	Ca,Mg,Si; Fe		
97	858	Cp	Ca,Na,Fe,Si; Cr,Ni	887	
	858	NZ			
98	740	Np			717-874
99	847	Cp	Ca,Fe,Si; Na	988	
100	924	Op	Fe,Si	1030	

Table 8

Calculated Liquidus Temperatures and Primary Phases for CVS Glasses

ID #	CVS #	Calculated		Tl spinel	Comments
		Tl	Phase		
1	1	907 850	ZS Cp	968	
2	2	920	CAS		Phase contains Ca, Si, Al as observed
3	3	970	Al_2O_3		X (poor agreement)
4	4	985	SO		
5	5	920	Cp	1062	Experimental "$FeSiO_3$" is an unstable compound
6	6	1116	ZS		
7	7	1155	ZS		
8	8	1201	ZS		
9	9	943	Mg_2BO_3	1273	Experimental marked "?"
10	10	—	—	997	
11	11	929	CAS	1111	Phase contains Ca, Si as observed
12	12	831	NCS2	946	Experimental "$FeSiO_3$" is an unstable ompound
13	13	---	---		
14	14	---	---		
15	15	859 873	Ov LS		Ov = Mg_2SiO_4
16	16	1153	Np		X (poor agreement) - See Note (a)
17	17	907 888	NCS1 Cp	1108	Phase contains Ca, Si as observed
18	18	1216 1113	Ov ZO		X (poor agreement) OK
19	19	907 850	ZS Cp		
20	20	907 850	ZS Cp		
21	21	985	SO		
22	22	1201	ZS		

ID #	CVS #	Calculated Tl Phase	Tl spinel	Comments
23	23	890 Cp -	993	
24	1	834 ZS	1065	X (poor agreement) - possible inprovement if Ni included in Ov model
25	2	871 Hm 870 Cp	1152	
26	3	894 ZS 835 Cp		
27	4	801 Cp		
28	5	814 Albite	982	Chemical analysis questionable. Small crystals and interference from glass
29	6	898 Cp		
30	7	770 Np	1116	X (poor agreement) - possible improvement if Ni included in Ov model
31	8	876 Cp		
32	9	1038 ZS		
33	10	--- ---	866	
34	11	1005 ZS		
35	12	817 Cp		
36	13	872 Cp		
37	14	1062 ZS		
38	15	--- ---	1001	
39	16	889 NZ 851 Cp	885	
40	17	907 ZS 850 Cp		
41	18	889 NZ 851 Cp		
42	19	890 NZ 853 Cp		
43	20	1081 ZS		
44	21	880 SO		X (poor agreement)
45	22	1004 Ov	915	
46	23	859 NCS1		Phase contains Ca, Si as observed

ID #	CVS #	Calculated Tl	Calculated Phase	Tl spinel	Comments
47	24	---	---	1011	
48	25	900	Cp		
49	26	1039	ZS		
50	27	---	---		
51	28	---	---		
52	29	1077	ZS		
53	30	898	Np	913	x (poor agreement)
54	31	897	SO		
55	32	1055	NZ		
56	33	969	Np	753	
57	34	1103	Np		X (poor agreement) - See Note (a)
58	35	971	Np	914	
59	36	909	Cp		
60	37	810	Np		
61	38	954	Np		X (poor agreement) - See Note (a)
62	39	996	NZ		
63	40	853	Cp		
64	41	907	Cp		
65	42	967	Cp	1018	
66	43	1057	ZS		
67	44	895 865	ZS Cp		See Note (b)
68	45	945 865	ZS Cp		See Note (b)
69	46	866 815	ZS Cp	1051	See Note (b)
70	47	914 840	NZ Cp		See Note (b)
71	48	798 781	ZS Cp		X (poor agreement) - problem could be related to high Cr and Ni contents of solid phases (not modeled)

ID #	CVS #	Calculated Tl	Phase	Tl spinel	Comments
72	49	818 815	Zs Cp	930	See Note (b)
73	50	907 850	ZS Cp		
74	51	890 884 853	NZ ZS Cp	889	
75	52	973	ZS		? (good T agreement)
76	53	---	---		
77	54	---	---		
78	55	1028	CO(R)	1124	CO(R) temperature will be lower if a significant amount of spinel precipitates first
79	56	963 884	CO(R) ZS	1124	If CO(R) precipitates in ID# 78, 80 then it must also precipitate here
80	57	995 853	CO(R) Cp	735	
81	58	944	LA		X poor agreement as regards phase
82	59	885 768	Np Cp		X (poor agreement) - See Note (a)
83	60	784 777	NZ Cp		Experimental observation of SO probably related to formation of two-phase liquid
84	61	782	Cp		Experimental observation of SO probably related to formation of two-phase liquid
85	62	---	---		
86	63	1215	Np		X (poor agreement) - See Note (a)
87	64	921 907	NZ Cp	957	See Note (b)
88	65	1122	ZS		
89	66	872	Np		
90	67	1025	CO(R)		
91	68	1732	CO(R)		
92	69	1663	CO(R)		
93	70	1481	CO(R)		

ID #	CVS #	Calculated Tl Phase	Tl spinel	Comments
94	71	921 NZ 907 Cp	929	? (satisfactory agreement in T)
95	72	872 Np		
96	73	851 Np 762 LA		
97	74	812 Cp	1123	
98	75	887 Np 774 LA		
99	76	892 Cp		X poor agreement in T (correct phase)
100	77	979 NZ		
101	78	1074 NZ		
102	79	847 SO		Phase correct. T too low
103	80	1133 ZS	1120	
104	81	879 Cp	901	Experimental marked "?"
105	82	796 NZ 734 Cp		T correct (experimental "LS" was a guess)
106	83	786 NCS2		Phase contains Ca, Si as observed
107	84	926 NZ		
108	85	949 Np		Experimental marked "?"
109	86	1140 Np		
110	87	--- ---		
111	88	903 NZ		
112	89	899 NZ 865 Cp		See Note (b)
113	90	815 Cp		
114	91	911 Albite 873 Np 820 SO	853	
115	92	963 ZS		
116	93	862 Cp	902	
117	94	932 Np 823 Cp		X (poor agreement) See Note (a)
118	95	870 Cp		

ID #	CVS #	Calculated TI	Calculated Phase	TI spinel	Comments
119	96	907 850	ZS Cp		
120	97	890 884 853	NZ ZS Cp		
121	98	1103 720	Np Albite		X (poor agreement) See Note (a)
122	99	876	Cp	949	
123	100	952 884	ZS Cp	1067	Experimental "$FeSiO_3$" is an unstable compound

Cp = clinopyroxene = $NaFeSi_2O_6$-$CaMgSi_2O_6$ solid solution
Hm = hematite Np = Nepheline Ov = Olivine
LA = Li-Al silicate LS = Li_2SiO_3 NZ = Na-Zr silicate
SO = SiO_2 ZO = ZrO_2 ZS = $ZrSiO_4$
CO(R) = Cr_2O_3-Fe_2O_3,Al_2O_3 (corundum) solid solution
CAS = $CaAl_2Si_2O_8$ (Anorthite)
NCS1 = $Na_2Ca_2Si_3O_9$-$Na_4CaSi_3O_9$ solid solution
NCS2 = $Na_2Ca_3Si_6O_{16}$

Note (a) In general, the precipitation of nephiline is poorly predicted because the optimization of the Na_2O-Al_2O_3-SiO_2 diagram is poor in this composition range. If nepheline is calculated as a primary phase, be skeptical.

Note (b) Glass contains low ZrO_2. Small amount of ZS or NZ precipitate could have been missed in experiments.

7.1 Discussion

Of the 17 compositions for which nepheline (Np) is the calculated primary phase, agreement between experimental and calculated liquidus temperatures is acceptable in only 9 cases. This is as expected from the discussion in Section 2.2. When nepheline is calculated as the primary phase, be skeptical.

In Fig. 1 are plotted experimental versus calculated liquidus temperatures for the 80 compositions (excluding the 17 compositions for which nepheline is calculated as the primary phase) for which experimental liquidus temperatures are given in Table 7. The average deviation is 32°. (If the 17 nepheline points are also included, the average is 47°) Eight of the eleven points for which experimental values were indicated as " > T " are also shown on Fig. 1. (The other three, ID #67-69 are off the scale of Fig. 1 but calculations agree with observations.)

In several glasses (ID# 67, 68, 69, 70, 72, 87, 112), Zr-containing phases (ZS or NZ) were calculated as primary phases. Although these were not observed experimentally, these glasses contain very low ZrO_2 contents, and the small amounts of precipitate could have been overlooked.

Orthopyroxene (Op), either as $MgSiO_3$ or a solution of $MgSiO_3$ and $FeSiO_3$, was never obtained as a primary phase in the calculations. Furthermore, its calculated thermodynamic activity was always very low. That is, only large changes in the optimized thermodynamic properties of this phase, well outside the error limits of the present calculations, would cause it to appear. Furthermore, in many cases, the experimental observations (Table 7) indicate an Op phase containing only Fe and Si. However, pure $FeSiO_3$ is an unstable compound. We thus have no explanation for the experimental observation of the Op phase.

In several cases, $CaSiO_3$(CS) is shown in Table 7 as the primery experimental phase. In the calculations, the thermodynamic activity of this phase was also always low. However, anorthite (CAS = $CaAl_2Si_2O_8$) or a sodium-calcium silicate (NCS1 or NCS2) were observed as primary phase in these samples, and these compounds contain the elements Ca, Si, (Al) observed by SEM/EDS.

Somewhat better agreement might be obtained by incorporating Ni into the models for some of the solid phases, particularly olivine. Unfortunately, there are few data upon which the modeling could be based.

CVS-II glasses #55-57 differ only in the content of Cr_2O_3(and MnO_2). Hence, if corundum (Cr_2O_3 solution) precipitates in #55 and 57, it would also be expected to precipitate in #56 as calculated, but this apparently was not observed.

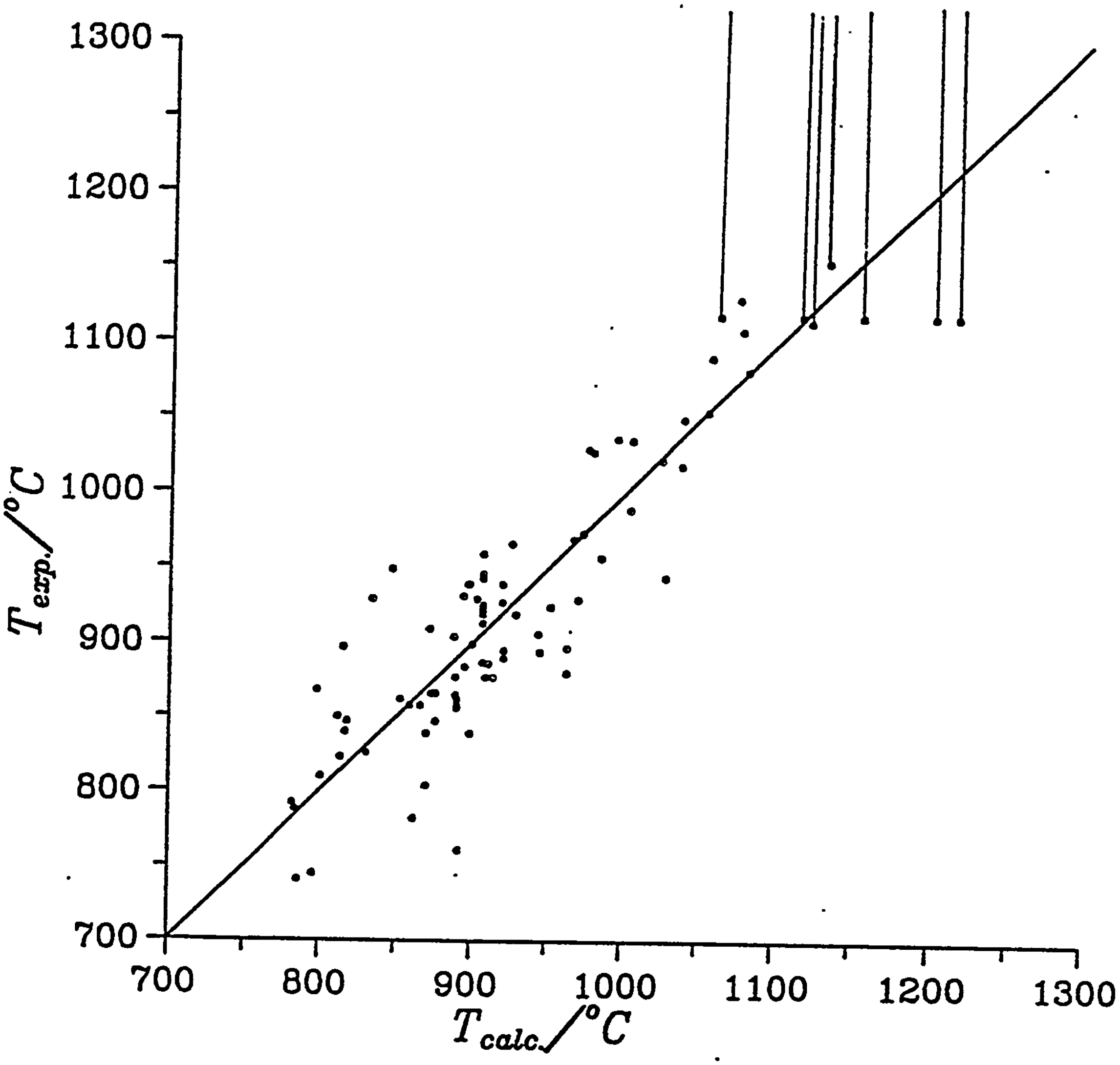

Comparison of Experimental and Calculated Liquidus Temperatures for CVS Glasses (Assuming negligible spinel precipitation)

Fig. 1

8 THE SPINEL PHASE

A two-sublattice model for (Fe, Ni)(Fe, Cr, Al)$_2$O$_4$ spinel solutions has been developed through optimization of available thermodynamic data for the pure components (Fe_3O_4, $NiCr_2O_4$, etc.) and of available data for equilibria between the spinel phase and other solid phases (corundum, wustite, metal, etc.) as a function of oxygen pressure, temperature and composition in the Fe-Cr-O, Fe-Ni-O, Fe-Al-O, Ni-Cr-O and Fe-Cr-Al-O systems.

Manganese was included in the spinel model by taking literature data for the pure compounds $MnAl_2O_4$ and Mn_3O_4, by taking ΔH°_{298} from the literature for the pure compounds $MnCr_2O_4$ and $NiMn_2O_4$ and then estimating S°_{298} and Cp by an increment method, and by using the observed fact that Mn_3O_4-Fe_3O_4 solid solutions are nearly ideal.

Good agreement with a large and diverse body of experimental data was obtained. It is thus believed that the thermodynamic properties of the spinel (Fe, Mn, Ni)(Fe, Mn, Cr, Al)$_2$O$_4$ phases are well modeled. Inaccuracies in calculations of spinel liquidus temperatures are more likely due to the database for the glass phase, or to the fact that the dissolution of Mg in the spinel solution was not modeled, or to the experimental results.

The spinel liquidus temperature was calculated for several CVS glasses for which observed spinel liquidus temperatures are reported in Table 7. Results of the calculations at $P_{O_2} = 1$ atm are shown in Table 8. The oxygen pressure had little effect. Decreasing p_{O_2} to 10^{-3} atm changed the calculated liquidus temperatures only by approximately 3°. A comparison of Tables 7 and 8 shows that agreement is satisfactory in some cases and poor in others. Out of 24 samples, an average deviation of 68° was obtained. Of 8 additional samples in which the experimental observations were shown as " > T ", agreement was found in 3.

In the case of samples with ID# 88 and 89 (CVS-II #55, 56), calculation of the spinel liquidus temperature before Mn was added to the spinel model gave Tl = 809°. That is, adding Mn to the spinel phase gives a large increase in the calculated temperature and results in much better agreement with the experimental results in these high-Mn(see Table 6) glasses.

9 SOLUBILITY OF SO_3, PO_4, Cl, F, I AND H_2O IN GLASSES

Recently we have developed a simple model [93 Pel] which has proved very successful in predicting the solubility of sulfur as sulfide ion, S^{2-} (under reducing conditions) in oxide slags and glasses for concentrations up to about 10 wt.%. It is assumed that the S^{2-} ions substitute nearly ideally for O^{2-} ions and for SiO_4 groups in the glass structure. Sulfide solubilities can then be predicted from a knowledge only of G° of the pure sulfides (Na_2S, CaS etc.) and of the activities of the oxides in the glass (which are given by the quasichemical model.) If necessary, constant adjustable parameters, $RT\ln\gamma_{MS}$(where γ = activity coefficient) may be included. The model has been described in detail [93 Pel] and its application to the calculation of sulfide solubilities has been demonstrated.

In the present study, the model has been adapted to permit the calculation of the solubility of other anions (SO_4^{2-}, Cl^-, I^-, F^-, PO_4^{3-}, OH^-) in an oxide slag or glass through substitution for O^{2-} ions or SiO_4 groups. This has required re-programming of a number of F*A*C*T software modules.

Under oxidizing conditions, sulfur dissolves in glass as sulfate. The dissolution can be written:

$$O^{2-} + SO_3 = SO_4^{2-}$$

For dilute solutions of SO_4^{2-}, the activity of the oxide ion is constant and the activity of SO_4^{2-} abeys Henry's Law. Hence, the weight of dissolved SO_4 (or dissolved "SO_3" or dissolved "S") varies directly as p_{SO_3}. Alternatively, the dissolution can be written as:

$$O^{2-} + SO_2 + 1/2\ O_2 = SO_4^{2-}$$

or as

$$O^{2-} + 1/2\ S_2 + 3/2\ O_2 = SO_4^{2-}$$

in which case the weight of dissolved sulfate varies as ($P_{SO_2}\ P_{O_2}^{1/2}$) or as ($P_{S_2}^{1/2}\ P_{O_2}^{3/2}$). This behavior has been observed, thereby confirming that under oxidizing conditions the predominant sulfur-containing species in solution is SO_4^{2-}.

The dissolution of phosphorus as phosphate under oxidizing conditions has been confirmed by the observation that the weight percent of dissolved phosphorus varies closely as ($P_{P_2}^{1/2}\ P_{O_2}^{5/4}$)according to the mechanism:

$$3/2\ O^{2-} + 1/2\ P_2 + 5/4\ O_2 = PO_4^{3-}$$

In the case of H_2O, it has been observed that the weight of dissolved H_2O varies as $P_{H_2O}^{1/2}$, thereby indicating dissolution as OH^- according to:

$$1/2\ O^{2-} + 1/2\ H_2O = OH^-$$

However, there is evidence that some of the hydroxyl groups are bonded to the silicon network. Therefore, the simple model has been modified in this case as discussed below in Section 9.4.

In the following sections, the model is used to calculate solubilities of sulfate, phosphate, halides and water, and the calculations are compared to the available data. In most cases, no adjustable parameters were required. The model calculations are probably valid to total solute concentrations of about 10 wt.%.

9.1 SO_3 Solubilities

For the case of sulfur solubility as SO_4^{2-} in glasses, no adjustable model parameters whatsoever were used. The G° values for Na_2SO_4, Li_2SO_4, $CaSO_4$ and $MgSO_4$ were taken directly from the F*A*C*T database. That is, the following comparisons with measured solubilities involved no curve-fitting, and are *a priori* predictions.

SO_3 solubilities in glasses in equilibrium with a gaseous phase have been reported by many authors. Nagashima and Katsura [73 Nag] measured SO_3 solubilities in Na_2O-SiO_2 melts at different SiO_2/Na_2O ratios at different temperatures for constant $P_{SO_2} P_{O_2}^{1/2} = 0.08$ kPa. Their results and calculated values are compared in Table 9. Similar measurements by Holmquist [66 Hol] are compared with calculated values in Table 10. In these experiments, $P_{SO_2} P_{O_2}^{1/2}$ was also varied and the expected approximately linear relationship between log(wt.% SO_3) and log $(P_{SO_2} P_{O_2}^{1/2})$ was observed. Papadopoulos [73 Pap] measured SO_3 solubilities in predominantly SiO_2-CaO-Na_2O glasses at $P_{SO_3} \approx 0.01$ atm. His results (corrected to $P_{SO_3} = 0.01$ atm) are compared to calculated values in Table 11. Fincham and Richardson's [54 Fin] measurements of SO_3 solubilities in CaO-Al_2O_3-SiO_2 glasses at 1500°C are compared to measurements in Table 12. Other data reported by these authors at 1650°C were not sufficiently complete to permit the calculation of SO_3 solubilities. However, relative solubilities among glasses of different compositions can be deduced from their results, and these are also compared with calculations in Table 12.

From Tables 9-12 it can be seen that agreement between experimental and calculated solubilities is good to excellent. The best agreement is with the results of Papadopoulos in Table 11. The agreement with the result of Holmquist in Table 10 is not as good at low SiO_2/Na_2O ratios, but any attempt to improve this agreement by introducing adjustable parameters results in poorer agreement with the other authors. That is, the agreement is believed to be within the error limits of the experiments.

Schreiber et al [87 Sch] measured SO_3 solubilities in an alkali borosilicate glass of composition (wt.%) 57.9 SiO_2, 1.0 TiO_2, 0.5 ZrO_2, 14.7 B_2O_3, 0.5 La_2O_3, 2.0 MgO, 5.7 Li_2O and 17.7 Na_2O. Results from the authors' smoothed curve are compared with calculated values in Table 13. (In the calculation, TiO_2 and La_2O_3 were ignored.) Agreement is within the range of scatter of the data points as reported in the article [87 Sch].

Table 9

Calculated SO_3 Solubility in Na_2O-SiO_2 Glasses Compared to Measurements of Nagashima and Katsura [73 Nag]

$(P_{SO_2}P_{O_2}^{1/2} = 0.08\ \mathrm{kPa})$

Molar Ratio (SiO_2/Na_2O)	T (°C)	1/T (10^{-4}/K)	ln W_{SO_3} (weight fraction)	
			expt.	calc
1	1300	6.36	-3.1	-2.7
	1250	6.57	-2.8	-2.3
	1100	7.28	-0.7	(-2.0)
2	1300	6.36	-6.3	-7.4
	1250	6.57	-5.8	-6.4
	1100	7.28	-2.9	-3.45
3	1300	6.36	-9.7	-9.9
	1250	6.57	-9.1	-8.9
	1100	7.28	-5.2	-5.5

Table 10

Calculated SO_3 Solubility in NaO_2O-SiO_2 Glasses Compared to Measurements of Holmquist [66 Hol]

T (°C)	(SiO_2Na_2O) Molar Ratio	$10^4 P_{SO_2} P_{O_2}^{1/2}$ (atm)	log (wt.% SO_3)	
			expt. (Smoothed)	Calc.
1150	2	0.3	-0.32	-0.24
		1	0.20	0.20
		3	0.69	0.52
	3	3	-0.26	-0.36
		10	(0.71)	0.10
	4	10	-0.22	-0.40
1200	1.5	1	0.76	0.54
		3	1.06	0.78
	1.75	1	0.47	0.15
		3	0.81	0.48
	2.0	1	0.05	-0.24
		3	0.46	0.16
		10	0.89	0.52
	2.5	1	-0.75	-0.85
		3	-0.22	-0.41
		10	0.36	0.05
	3	3	-0.86	-0.85
		10	-0.31	-0.34
		30	0.16	0.08
	4	10	-0.84	-0.89
		30	-0.25	-0.41
1250	1.5	1	0.48	0.20
	1.75	1	0.00	-0.28
	2	1	-0.27	-0.69
		3	0.02	-0.24
		10	0.35	0.19
		30	0.85	0.52
	2.5	10	-0.15	-0.37
	3	10	-0.61	-0.78
		30	-0.16	-0.33

Table 11

Calculated SO_3 Solubilities in SiO_2-CaO-Na_2O-(Al_2O_3-MgO) Glasses Compared to Measurements of Papadopoulos [73 Pap]

(at P_{SO_3} = 0.01 atm)

T (°C)	Mole fractions					SO_3(mole fraction)	
	SiO_2	Al_2O_3	CaO	MgO	Na_2O	expt. (corrected)	calc.
1370	0.721	0.002	0.136	0.005	0.127	0.00745	0.00715
	0.722	0.001	0.142	0.004	0.123	0.00636	0.00685
	0.741	0.001	0.089	0.003	0.159	0.00664	0.0103
	0.707	0.001	0.200	0.005	0.083	0.00280	0.00417
	0.715	0.001	0.193	0.005	0.083	0.00280	0.00385
	0.710	0.001	0.196	0.005	0.085	0.00238	0.00420
	0.653	0.002	0.195	0.005	0.133	0.01216	0.0162
	0.653	0.002	0.196	0.004	0.132	0.01265	0.0161
	0.657	0.002	0.194	0.005	0.131	0.01050	0.0151
	0.661	0.002	0.195	0.005	0.127	0.00967	0.0137
	0.685	0.002	0.144	0.004	0.154	0.01066	0.0156
	0.778	0.001	0.090	0.004	0.123	0.00360	0.0044
	0.778	0.001	0.144	0.004	0.071	0.00133	0.00185
1373	0.653	0.002	0.196	0.004	0.132	0.0126	0.0157
1397	0.660	0.002	0.198	0.005	0.128	0.0115	0.0108
1403	0.659	0.002	0.194	0.004	0.131	0.0107	0.0108
1427	0.677	0.002	0.187	0.005	0.123	0.0066	0.0060
1433	0.669	0.002	0.192	0.004	0.128	0.0062	0.0069
1451	0.660	0.002	0.201	0.005	0.128	0.0063	0.0063
1453	0.665	0.002	0.194	0.006	0.129	0.0050	0.0058
1483	0.666	0.002	0.199	0.005	0.125	0.0038	0.0040

Table 12

Calculated Sulphate Capacities, C_{SO_4}, of CaO-Al_2O_3-SiO_2 Glasses Compared to Measurements of Fincham and Richardson [54 Fin]

$$C_{SO_4} = (\text{Wt.\% } S/P_{S_2}^{1/2}\ P_{O_2}^{3/2}) \text{ where } P = \text{atm.}$$

Slag Number [54 Fin]	Composition (wt.%)			log C_{SO_4} at 1500°C	
	CaO	Al_2O_3	SiO_2	expt.	calc
S1	37	27	36	6.70	6.43
S2	32.5	26.5	41	6.50	5.94
S4	54	1	45	7.18	7.02
S5	41	52	7	7.83	7.60
S6	45.8	18	36.2	7.20	7.05
				log C_{SO_4} - log C_{SO_4} (slag 56) at 1650°C	
				expt.	calc.
S11	54	0	46	-0.25	-0.03
S12	48	0	52	-0.35	-0.46
S14	35.5	64.5	0	-0.20	0.22
S15	41	59	0	0.15	0.63
S16	52.5	47.5	0	0.95	1.33

Table 13

Calculated SO_3 Solubility in Alkali Borosilicate Glass at 1150°C Compared to Measurements of Schreiber et al [87 Sch]

log ($10^4\ P_{SO_2}\ P_{O_2}^{1/2}$) (atm)	log (wt.% S)	
	expt. (smoothed)	calc.
1.0	-0.44	-0.77
1.5	0.03	-0.32

Table 14

Calculated SO_3 Solubilities in Glass in Equilibrium with a Molten Salt Phase for Glass Compositions used by Sullivan [94 Sull]

Glass Compositions (wt. %)

	WL-3	WL-4	WL-5
SiO_2	59.2	57.1	55.0
B_2O_3	11.4	10.8	10.3
Na_2O	11.2	11.2	11.2
Li_2O	6.8	6.8	6.8
Al_2O_3	6.2	7.6	9.1
P_2O_5	1.1	1.4	1.6
SO_3	1.3	1.6	1.9
Others	2.8	3.5	4.1

SO_3 Solubilities in Glass in Equilibrium with Liquid Na_2SO_4-Li_2SO_4 Solution

Glass	T (°C)	wt.% SO_3 in glass	wt.% Li_2SO_4 in equilibrium molten salt phase
WL-3	900	0.95	9.8
	1150	1.36	13.7
	1400	1.51	16.9
WL-4	900	0.95	9.3
	1150	1.37	13.1
	1400	1.56	16.4
WL-5	900	0.93	8.8
	1150	1.39	12.6
	1400	1.61	15.9

Table 15

Base Composition of Simulated Low Level Nuclear Waste Glass Used in Studies of Crichton et al [94 Cri]

Component	wt.%	Component	wt.%	Component	wt.%
SiO_2	56.78	P_2O_5	1.187	Fe_2O_3	0.005
B_2O_3	5.00	F	0.213	Cr_2O_3	0.036
Na_2O	20.00	Cl	0.092	Nd_2O_3	0.012
Al_2O_3	12.00	SO_3	0.321	Bi_2O_3	0.014
CaO	4.00	K_2O	0.327	ZrO_2	0.005

SO_3 solubilities in glass in equilibrium with a molten sulfate phase have also been reported. Kordes et al [51 Kor] (quoted by [66 Hol]) reports solubilities of Na_2SO_4 of 7 and 3 wt.% in $Na_2O{\bullet}2SiO_2$ and $Na_2O{\bullet}3SiO_2$ respectively at 1200°C in equilibrium with liquid Na_2SO_4. Calculations give 9.4 and 4.8 wt.% respectively. Pearce and Beisler [65 Pea] indicate a composition containing ~ 3 wt.% Na_2SO_4 at the glass/tridymite/Na_2SO_4(liq.) triple point at 1200°C. Calculations give 2.6 wt.%.

For the three alkali borosilicate glass compositions listed in Table 14, Sullivan [94 Sul] reports a solubility of SO_3 (in equilibrium with a molten sulfate phase) of 1.3 wt% SO_3 for glass WL-3 and 1.1 and 1.2 wt.% for glasses WL-4 and WL-5 respectively, without specifying the temperature. Calculated solubilities in Table 14 are in very good agreement with the results of Sullivan. It can be seen that the calculated solubilities are quite insensitive to temperature (as expected for equilibrium between two liquid phases).

Finally, Crichton et al [94 Cri] report a "solubility" of 0.68 wt.% SO_3 in equilibrium with Na_2SO_4 (temperature unspecified) for an alkali borosilicate glass of the composition given in Table 15. Calculations (ignoring minor constituents) gave 2.4, 2.2 and 2.1 wt% SO_3 at 900°, 1150° and 1400°C respectively. This agreement is not as good, but the description of the experimental method as given by Crichton et al is not at all clear.

9.2 Phosphate solubilities

For phosphate solubilities in glasses there are very few measurements, and these are often contradictory and of poor accuracy. The thermodynamic properties of the pure phosphates are also not well known.

Thermodynamic data for pure liquid $Mg_3(PO_4)_2$ were taken from the F*A*C*T database. Data for solid $Ca_3(PO_4)_2$ and $Na_3(PO_4)$ were found, but no data for the liquids were found and so these were estimated from the solid data and from estimated Gibbs energies of fusion. For $Li_3(PO_4)$, only the enthalpy of formation at 298 K was found. Properties of the liquid were estimated by assuming that ΔS and ΔCp for formation of $Li_3(PO_4)$ from Li_2O and P_2O_5 are the same as for the formation of $Na_3(PO_4)$ from Na_2O and P_2O_5.

No adjustable model parameters were used.

Crichton et al [94 Cri] report a solubility limit of 3.0 wt.% P_2O_5 in a glass of the composition given in Table 15 when in equilibrium with pure solid Na_3PO_4 and $Na_2Ca_4(PO_3)_2SiO_4$. They do not indicate the temperature for this result, and the description of their experiment is not clear. Calculations give P_2O_5 contents at 700°, 900°, 1100°, 1300° and 1500°C of 0.13, 0.74, 1.98, 2.9 and 3.8 wt.% respectively in equilibrium with solid $Na_3(PO_4)$ and $Ca_3(PO_4)_2$.

Phosphate solubilities in Na_2O-SiO_2 glasses in equilibrium with a gas phase are reported by Inoue and Suito [85 Ino]. These are reported as "phosphate capacities", $C_{PO_4} = (\text{wt.\% } PO_4)/P_2^{1/2} \bullet P_{O_2}^{5/4}$ (p = atm). At 1250°C in solutions with SiO_2/Na_2O molar ratios of 3/2 and 1/1, values of $\log(C_{PO_4}) = 26.4$ and 25.4 respectively are reported, whereas present calculations give 27.2 and 24.6 respectively as shown in Table 16. Similar data from other sources have been collected by Ban-ya and Hino [91 Ban]. Discrepancies of this order are found between sources.

The calculated temperature dependence of C_{PO_4} over the range 1200° to 1350°C agrees well with the reported data [91 Ban].

Inoue and Suito [85 Ino] report phosphate capacities for Na_2O-SiO_2 glasses with additions of Mg and Ca silicates. These are shown in Table 16 where it can be seen that agreement with calculated values is satisfactory.

Table 16

Calculated Phosphate Capacities C_{PO_4} in Glasses at 1250°C Compared with Measurements of Inoue and Suito [85 Ino]

$$C_{PO_4} = (\text{wt.\% } PO_4/P_{P_2}^{1/2}\ P_{O_2}^{5/4})\ \text{where } P = \text{ atm}$$

Composition (wt.%)			log (C_{PO_4})	
$3Na_2O \cdot 2SiO_2$	$3CaO \cdot 2SiO_2$	$3MgO \cdot 2SiO_2$	expt.	calc.
100	0	0	26.4	27.2
80	20	0	26.2	26.4
80	0	20	25.7	24.3
$Na_2O \cdot SiO_2$	$CaO \cdot SiO_2$	$MgO \cdot SiO_2$		
100	0	0	25.4	24.6
80	20	0	24.85	24.1
80	0	20	24.7	23.5

9.3 Halide solubilities

The only data which could be found on the solubilities of halides are those of Crichton et al [94 Cri]. As already mentioned above, the descriptions of the experiments are confusing, and in the case of sulfate solubilities Crichton et al do not agree well with Sullivan [94 Sul] who studied glasses of similar composition.

For the model calculations, all G° values of the pure halides were taken from the F*A*C*T database.

For the case of chloride solubilty, no adjustable model parameters were required. At 900°C, 1100°C and 1300°C, the Cl content of a glass of the composition given in Table 15 (ignoring minor components) was calculated as 0.77, 0.78 and 0.79 wt% respectively when in equilibrium with liquid NaCl. Crichton et al, without giving a temperature, report a solubility of 0.8 wt.% in excellent agreement with the calculations. The insensitivity of the solubility to change in temperature is as expected for equilibrium between two liquid phases. Crichton et al also report solubilities as a function of temperature over the range 800°C to 1300°C, but it is not possible to decipher from their description exactly what they measured nor exactly what the results were. In any case, they observed the solubility to be insensitive to temperature changes, in agreement with the calculations.

For the case of iodide solubility, Crichton et al report solubilities of 0.5 ± 0.3 wt.% I (depending on the experimental method) when a slag of the composition of Table 1 is in equilibrium with liquid NaI. With no adjustable model parameters, a solubility of ~ 2.0 % was calculated. An adjustable parameter of $RT\ln\gamma_{NaI}$ = 3500 cal/mol was thus introduced, resulting in calculated solubilities of 0.37, 0.53 and 0.69 wt.% at 700°, 900° and 1100°C respectively. Such a small positive parameter is reasonable in view of the large size of the iodide ion which would tend to decrease its solubility. Similar parameters $RT\ln\gamma_i$ = 3500 cal/mol were also included for $Ca_{1/2}I$, LiI and $Mg_{1/2}I$ in the glass.

For the case of fluoride solubility, the glass is in equilibrium with solid fluorides over the temperature range of the experiments of Crichton et al. Hence, the solubility will depend more strongly on temperature. These authors report a solubility of 2.8 wt.% F in a slag of the composition given in Table 15. This seems to be the value observed at 725°C (see their figure 2). With no adjustable parameters, a solubility of 0.6 wt.% was calculated at 725°C in equilibrium with solid NaF and solid CaF_2. Accordingly, an adjustable parameter of $RT\ln\gamma_{NaF}$ = -3500 cal/mol was introduced, resulting in a calculated solubility of 2.65 wt.% at 725°C. Such a small negative parameter is reasonable in view of the fact that fluorine can probably enter the glass not only as F^- ions but also by bonding directly to Si, thereby increasing its solubility. Similar parameters $RT\ln\gamma_{NaF}$ = -3500 cal/mol were also included for $Ca_{1/2}I$, LiI and $Mg_{1/2}I$ in the glass.

The calculations give a solubility of 8.7 mol % F (2.65 wt.% F) at 725°C and 10.1 mol % F at 850°C in equilibrium with solid NaF and CaF_2. Crichton et al, in their figure 2, show an "immiscibility boundary" of 8.9 mol % at 725°C and ~13.5 mol % at 850°C. However, the interpretation of this figure, and how it was obtained, are unclear.

9.4 H_2O Solubilities

In basic glasses, water is presumed to dissolve principally as free OH^- ions. However, in acid glasses, the hydroxyl groups are most likely bonded to silicon (-Si-O-H). This is evidenced by the observation in several binary glass systems SiO_2-M_2O(M = Li, Na, K), SiO_2-CaO, etc. that as the SiO_2 content is increased the H_2O solubility at first decreases, but then passes through a minimum to increase again at high SiO_2 contents.

For the fraction which dissolves as free OH^- ions, the same model was used as was used for sulfate, phosphate and halide solubilities. For the fraction which dissolves as bonded hydroxy ions, a species "H_2O", formally similar to Na_2O, was introduced into the quasichemical model (with a quasichemical "charge parameter" of 0.3444).

Solubilities of H_2O in different binary glasses have been measured by several authors. These are generally in good agreement and have been compiled by Ban-ya and Hino [91 Ban]. Some representative results are shown in Table 17. The following model parameters were chosen so as to optimize these data: G° of liquid NaOH and KOH were taken from the F*A*C*T database. G° of liquid $Ca(OH)_2$ and $Mg(OH)_2$ were set equal to the values of the corresponding solids from the F*A*C*T database. The following adjustable parameters were then introduced: $RT\ln\gamma_i$ = -5.4, -18.0, -13.0 and -13.0 kcal/mol for i = NaOH, LiOH, $Ca_{1/2}OH$ and $Mg_{1/2}OH$ respectively. For pure H_2O, G° was set equal to the value obtained by extrapolating G° of liquid H_2O to high temperature and adding 30.0 kcal/mol. This is, of course, necessarily an adjustable parameter of the model, but this procedure was chosen so as to give a reasonable temperature dependence. Finally, the following optimized quasichemical parameters were introduced:

$$\omega_{HO_{1/2}SiO_2} = -22.0\ kcal/mol$$
$$\omega_{HO_{1/2}AlO_{3/2}} = -22.0\ kcal/mol$$

Calculated H_2O solubilities are compared with reported values in Table 17 for binary glasses and with values for a ternary glass in Table 18.

Table 17

Calculated H_2O Capacities, C_{H_2O}, of Binary Glasses Compared to Measurements

$$C_{H_2O} = (\text{wt.\% } H_2O/P_{H_2O}^{1/2}) \text{ where } P = \text{atm}$$

System	Mole Fraction X_{SiO_2} or $X_{Al_2O_3}$	T°C	log C_{H_2O}		ref.
			expt. (smoothed)	calc.	
Na_2O-SiO_2	0.85	1317	-0.96	-1.10	[58 Kur]
	0.80		-1.10	-1.15	
	0.75		-1.12	-1.24	
	0.70		-1.08	-1.36	
	0.50		-0.69	-0.69	
Li_2O-SiO_2	0.80	1300	-0.90	-1.19	[58 Kur]
	0.69		-0.97	-1.13	
	0.50		(-0.65)	-0.59	
	0.667	1394	-0.96	-1.05	[57 Rus]
		1156	-1.14	-1.15	
		977	-1.30	-1.23	
CaO-SiO_2	0.6	1600	-1.19	-1.15	[69 Igu]
	0.5		-1.21	-1.20	
	0.4		-1.05	-1.02	
CaO-Al_2O_3	0.5	1650	-1.00	-1.37	[90 Wat]
	0.4		-0.84	-0.80	
	0.3		-0.55	-0.42	

Table 18

Calculated H_2O Capacities, C_{H_2O}, of SiO_2-MgO-CaO Glasses at 1450°C with $X_{SiO_2} = 0.50$ Compared to Measurements of Ban-ya et al [86 Ban]

$$C_{H_2O} = (\text{wt.\% } H_2O/P_{H_2O}^{1/2}) \text{ where } P = \text{atm}$$

Molar Ratio MgO/(MgO + CaO)	log C_{H_2O}	
	expt.	calc.
0.25	~(-1.13)	-1.16
0.375	-1.12	-1.14
0.50	-1.10	-1.12
0.625	-1.08	-1.10
0.75	~(-1.05)	-1.07

10 MOLTEN SALT DATABASES

Databases have been developed for molten salt solutions which can exist in equilibrium with glasses. A sublattice model was used which has been described previously [88 Pel]. Databases were developed by optimization of thermodynamic and phase diagram data for all binary and several common-ion ternary systems. Many of these optimizations have been described in publications [87San, 88Pel, 90Des1, 90Des2, 90Des3, 91San] and several others have been more recently performed. In general, the model for molten salts is good, the optimizations reproduce the data very well, and there are many data available. Hence, the thermodynamic properties of the molten salt solutions are expected to be well modeled.

Two solution databases should be used in the calculations. The first, developed as a private database for Battelle, is the Li, Na, Mg, Ca/F,SO_4 solution. That is, this database models a molten salt solution containing the cations Li^+, Na^+, Mg^{2+}, and Ca^{2+} and the anions F^- and SO_4^{2-}. The other solution is the F*A*C*T public solution database /SOLN-SALT/ which models the Li, Na/F, Cl, I, SO_4 molten phase.

11 REFERENCES

[30 Bow] N.L. Bowen, J. F. Schairer and H.W.V. Willems, Am. J. Sci., 20, 405-455 (1930).

[51 Kor] E. Kordes, B. Zöfelt and H. Pröger, Z. Anorg. Allg. Chem., 264, 255-271 (1951).

[51 Mor] G.W. Morey, J. Soc. Glass Tech., 35, 270-284 (1951).

[54 Fin] C.J.B. Fincham and F.D. Richardson, Proc. Roy. Soc. London, A223, 40-62 (1954).

[57 Rus] L.E. Russell, J. Soc. Glass Tech., 41, 304T (1957).

[58 Kur] C. R. Kurkjian and L.E. Russell, J. Soc. Glass Tech., 42, 130T (1958).

[60 Osb] E. F. Osborn and A. Muan, "Phase Equilibrium Diagrams of Oxide Systems", Am. Ceram. Soc. (1960).

[65 Pea] M.L. Pearce and J.F. Beisler, J. Am. Ceram. Soc., 48, 40-42 (1965).

[66 Hol] S. Holmquist, J. Am. Ceram. Soc., 49, 467-473 (1966).

[69 Igu] Y. Iguchi, S. Ban-ya and T. Fuwa, Trans. ISIJ, 9, 189 (1969).

[73 Nag] S. Nagashima and T. Katsura, Bull. Chem. Soc. Jap., 46, 3099-3103 (1973).

[73 Pap] K. Papadopoulos, Phys. Chem. Glasses, 14, 60-65 (1973).

[85 Ino] R. Inoue and H. Suito, Trans. ISIJ, 25, 118 (1985).

[86 Ban] S. Ban-ya, Y. Iguchi and S. Yamamoto, Tetsu-to-Hagané, 72, 2210 (1986).

[87 San] J. Sangster and A.D. Pelton, J. Phys. Chem. Ref. Data, 16, 509-561 (1987).

[87 Sch] H.D.Schreiber, S. Kozak, P.G. Leonhard and K.K. McManus, Glastech. Ber., 60, 389-398 (1967).

[88 Pel] A.D. Pelton, Calphad J., 12, 127-142 (1988).

[90 Des1] Y. Dessureault, J. Sangster and A.D. Pelton, J. Electrochem, Soc., 137, 2941-2950 (1990).

[90 Des2] Y. Dessureault, J. Sangster, and A.D. Pelton, J. Phys. Chem. Ref. Data, 119, 1149-1178 (1990).

[90 Des3] Y. Dessureault, J. Sangster and A.D. Pelton, J. Chim. Phys., 87, 407-453 (1990)..

[90 Hol] Holland and Powell, J. Metamorph. Geol., 8, 89-124 (1990).

[90 Wat] M. Watanabe, Y. Iguchi and S. Ban-ya, Tetsu-to-Hagané, 76, 1672 (1990).

[91 Ban] S. Ban-ya and M. Hino, "Chemical Properties of Molten Slags", Iron and Steel Inst. Japan, Tokyo(1991).

[91 San] J. Sangster and A.D. Pelton, J. Phase Equilib., 12, 511-537 (1991).

[92 Pel] A.D. Pelton, P. Wu and G. Eriksson, "Development of Models and Software for Liquidus Temperatures of Glasses of HWVP Products, "Report to Battelle, (November, 1992).

[93 Pel] A.D. Pelton, G. Eriksson and J. A. Romero-Serrano, Metall. Trans., 24B, 817-825 (1993).

[94 Cri] S.N. Crichton, T. J. Barbieri and M. Tomozawa, "Solubility Limits for Troublesome Components in a Simulated Low Level Nuclear Waste Glass", manuscript communicated by P. Hrma (1994).

[94 Sul] G.K. Sullivan, "Sulfate Segregation in Vitrification of Simulated Hanford Nuclear Waste Glass", manuscript communicated by P. Hrma (1994).